Consistent bosonization-debosonization. II. The two-lead Kondo problem and the fate of its nonequilibrium Toulouse point

C. J. Bolech and Nayana Shah
Department of Physics, University of Cincinnati, Cincinnati, Ohio 45221-0011, USA
(Received 13 August 2015; revised manuscript received 22 November 2015; published 29 February 2016)

Following the development of a scheme to bosonize and debosonize consistently [N. Shah and C. J. Bolech, Phys. Rev. B **93**, 085440 (2016)], we present in detail the Toulouse-point analytic solution of the two-lead Kondo junction model. The existence and location of the solvable point is not modified, but the calculational methodology and the final expressions for observable quantities change markedly as compared to the existent results. This solvable point is one of the remarkably few exact results for nonequilibrium transport in correlated systems. It yields relatively simple analytical expressions for the current in the full range of temperature, magnetic field, and voltage. It also shows precisely, within the limitations of the Toulouse fine-tuning, how the transport evolves depending on the relative strengths of interlead and intralead Kondo exchange couplings ranging from weak to strong. Thus its improved understanding is an important stepping stone for future research.

DOI: 10.1103/PhysRevB.93.085441

I. INTRODUCTION

In the first part of this series [1], we introduced a consistent prescription in order to be able to bosonize, make transformations, and debosonize consistently in the presence of "active local impurities or boundaries," which we called the consistent bosonization-debosonization (BdB) program. In this paper we explore the implications of this formalism for the important case of quantum impurity problems.

Just over fifty years ago, in 1964, Kondo showed that a mysterious finite-temperature minimum in the resistivity of metals was due to the contributions from dilute magnetic impurities present in the samples [2]. This marked the start of the study of the so-called *Kondo problem*, which is one of the pillars of modern condensed-matter theory [3]. On the technical side, the reason for this is that the problem of a single magnetic impurity in a metal is one of the very first examples of an asymptotically free theory [4]. When the system is below a certain energy scale known as the Kondo temperature, standard perturbation theory fails and one needs to resort to more sophisticated theoretical tools (many of which were actually first developed studying this problem [5]). These range from the exact to the versatile, or from the Bethe ansatz [6–10] to auxiliary-particle perturbation methods [11–15]. On the application side, the relevance of the Kondo problem extends nowadays well beyond the original system of impurities in metals. The so-called Kondo lattice is the central model in the study of heavy fermions [4] and, even more generally, a formalism know as dynamical mean field theory is based on the mapping of any complicated tight-binding model of a material to an effective quantum impurity problem [16]. Moreover, since the last two decades, as the study of artificial mesoscopic systems reached the nanoscale, the Kondo problem can show up in all sorts of electronic devices, most notably in semiconductor quantum dots [17,18] but also in molecular electronics [19], etc.

The experiments with artificial nanostructures brought in an additional layer of complication to the theory of the Kondo effect. Most of the typical experiments involve transport measurements in nonequilibrium conditions, while our best theoretical tools to describe systems out of equilibrium are perturbative. Since the Kondo effect is nonperturbative, a lot of theoretical activity continues to ensue, to the point that it is fair to say that a deep understanding of correlated systems out of equilibrium is still work in progress.

Early on during the nanoscale revolution in mesoscopics, the pioneering theoretical work of Schiller and Hershfield (S&H) provided the first (and still now one of the few) exact solution of a nonequilibrium strongly correlated quantum problem [20]. A few years before them, Emery and Kivelson (E&K) found a solvable point (called a Toulouse point) for the two-channel Kondo model [21] (in which, besides spin, the band electrons have one more two-valued discrete degree of freedom [22]). S&H realized that they could adapt it to the case of a Kondo impurity interacting with two separate leads. They thus found a mapping that allows for the calculation of transport in a problem that has strong correlations due to the exchange interaction between the electrons and the impurity spin. We will revisit the central aspects of their work below. We shall find that while the key insights of S&H about the existence of a nonequilibrium Toulouse point remain valid, our generic consistent-debosonization procedure shows that the actual observables being calculated are substantially modified and yield more physically consistent results.

II. MODEL OF A KONDO JUNCTION

We shall be interested in a class of systems in which the transport between two leads or terminals happens across a microscopic region in which the fermionic degrees of freedom are such that the region has a total magnetic moment that remains unscreened (and we will focus on the case of spin-1/2). This situation is typical of nano-scale quantum dots with strong Coulomb blockade and has been an experimental reality since the late 1990s [17,18]. At low temperatures, remarkably, the system enters the so-called Kondo regime and is able to conduct despite the Coulomb blockade.

We are thus interested in the low-temperature characteristics of nonlinear transport across a quantum dot in the Kondo

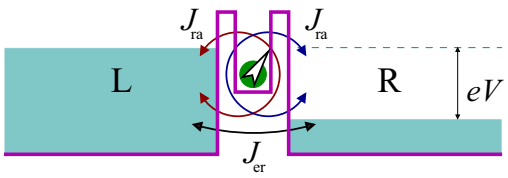

FIG. 1. Schematic depiction of the setting in which two Fermi seas kept at different chemical potentials with their difference given by $eV = \mu_L - \mu_R$ are connected via quantum tunneling across the potential barrier that separates them. The situation when the barrier region does not allow for internal states was discussed before [1]. Here there exists a many-body state trapped by the barrier with an unscreened total spin 1/2 that we refer to as the impurity (depicted by an arrowhead). Due to a strong Coulomb blockade, the impurity interacts with the electrons in the leads via exchange processes only. For the purpose of the figure we generically denote by J_{ra} the intralead exchange terms (either parallel or perpendicular) and by J_{er} the interlead cotunneling exchange processes that can give rise to a current (a similar notation will be introduced in the text later).

regime. We will model the system with a two-lead version of the Kondo model (see Fig. 1). In analogy to the equilibrium case, this model can be derived from a more microscopic Anderson-type model via a (time-dependent) Schrieffer-Wolff transformation [5,23]. In Hamiltonian language, the model is given by

$$H = \sum_{\sigma,\ell}\left(\int \mathcal{H}^0_\ell\, dx + H^z_K + H^\perp_K\right) + H_{\rm field}\,, \tag{1a}$$

$$\mathcal{H}^0_\ell = \psi^\dagger_{\sigma\ell}(x,t)(-i v_F\partial_x)\psi_{\sigma\ell}(x,t), \tag{1b}$$

$$H^z_K = J^z_{\ell\ell'}\, S^z_{\rm imp}\left(\frac{\sigma}{2}\psi^\dagger_{\sigma\ell}(0,t)\psi_{\sigma\ell'}(0,t)\right), \tag{1c}$$

$$H^\perp_K = J^\perp_{\ell\ell'}\, S^\sigma_{\rm imp}\left(\tfrac{1}{2}\psi^\dagger_{\bar\sigma\ell}(0,t)\psi_{\sigma\ell'}(0,t)\right), \tag{1d}$$

$$H_{\rm field} = -h\, S^z_{\rm imp}\,, \tag{1e}$$

where $\psi_{\sigma\ell}(x,t)$ are chiral fermions in the Heisenberg representation that are obtained after unfolding the two leads in the usual way [1,24]. We adopt the notation $\sigma = \{\downarrow,\uparrow\} = \{-1,+1\}$ and $\ell = \{L,R\} = \{-1,+1\}$ for the spin and lead index, respectively. The bar notation denotes a sign change—e.g., $\bar\sigma = -\sigma$. The impurity is described by $S^z_{\rm imp}$ and $S^\sigma_{\rm imp} = S^x_{\rm imp} + i\sigma S^y_{\rm imp}$. We assume now that at a much earlier time the connection between the two leads was established and that there is a battery keeping a constant chemical-potential difference between the two leads (what we call a Landauer-type configuration [25,26]). Under these conditions the system will be in a nonequilibrium steady state [27]. Let us call μ_ℓ the chemical potential of lead ℓ, such that $\mu_L - \mu_R = eV$, with V the voltage drop across the junction. The information about these chemical potentials will enter into the distribution functions for each lead.

III. BOSONIZATION-DEBOSONIZATION APPROACH

To set the stage for the bosonization of the model, we start by gauging away the chemical-potential difference. For that, let us first switch to Lagrangian language in which the system is described by

$$\mathcal{L}^0_\ell = \psi^\dagger_{\sigma\ell}(x,t)(i\partial_t)\psi_{\sigma\ell}(x,t) - \mathcal{H}^0_\ell$$
$$= \psi^\dagger_{\sigma\ell}(x,t)(i\partial_t + i v_F\partial_x)\psi_{\sigma\ell}(x,t), \tag{2a}$$

$$L^z_K = -H^z_K = -J^z_{\ell\ell'}\, S^z_{\rm imp}\left(\frac{\sigma}{2}\psi^\dagger_{\sigma\ell}(0,t)\psi_{\sigma\ell'}(0,t)\right), \tag{2b}$$

$$L^\perp_K = -H^\perp_K = -J^\perp_{\ell\ell'}\, S^\sigma_{\rm imp}\left(\frac{1}{2}\psi^\dagger_{\bar\sigma\ell}(0,t)\psi_{\sigma\ell'}(0,t)\right). \tag{2c}$$

We can now make the following (gauge) field transformation $\psi_{\sigma\ell}(x,t) = e^{-i\mu_\ell t}\check\psi_{\sigma\ell}(x,t)$. The important point is that now the distribution functions do not contain information about the chemical potentials any longer (cf. with the discussion for the case of a simple junction [1]). Next we subtract the vev (vacuum expectation value), which for a noninteracting problem is equivalent to factoring out the fast oscillations in each lead according to $\check\psi_{\sigma\ell}(x,t) = e^{ik^\ell_F x}\check\psi_{\sigma\ell}(x,t)$, with $k^\ell_F = \mu_\ell/v_F$ for this linear-dispersion case. So we are naturally, thanks to the linear dispersion, lead to the normal-ordered formulation of the problem:

$$\mathcal{L}^0_\ell = :\check\psi^\dagger_{\sigma\ell}(x,t)(i\partial_t + i v_F\partial_x)\check\psi_{\sigma\ell}(x,t):\,, \tag{3a}$$

$$L^z_K = -J^z_{\ell\ell}\, S^z_{\rm imp}\left(\frac{\sigma}{2} :\check\psi^\dagger_{\sigma\ell}(0,t)\check\psi_{\sigma\ell}(0,t):\right)$$
$$- e^{i\bar\ell eVt} J^z_{\ell\bar\ell}\, S^z_{\rm imp}\left(\frac{\sigma}{2}\check\psi^\dagger_{\sigma\ell}(0,t)\check\psi_{\sigma\bar\ell}(0,t)\right), \tag{3b}$$

$$L^\perp_K = -J^\perp_{\ell\ell}\, S^\sigma_{\rm imp}\left(\tfrac{1}{2}\check\psi^\dagger_{\bar\sigma\ell}(0,t)\check\psi_{\sigma\ell}(0,t)\right)$$
$$- e^{i\bar\ell eVt} J^\perp_{\ell\bar\ell}\, S^\sigma_{\rm imp}\left(\tfrac{1}{2}\check\psi^\dagger_{\bar\sigma\ell}(0,t)\check\psi_{\sigma\bar\ell}(0,t)\right). \tag{3c}$$

Notice that in the case of the *parallel* intralead impurity terms we wrote them also as normal ordered (since the vev's of the two spin projections cancel each other due to the $\sigma/2$ factor), which is customary in other approaches such as boundary conformal field theory (BCFT), whereas the interlead impurity terms naturally remain non-normal-ordered. At this point we lost the information about the absolute energy reference but we still have the information about the potential drop encoded in the time-dependent phase of the tunneling term.

A. Bosonization and initial mappings

The first part of the BdB program starts by bosonizing, of course. In order to do that, we go back to the Hamiltonian formulation of the problem,

$$\mathcal{H}^0_\ell = :\check\psi^\dagger_{\sigma\ell}(x,t)(-i v_F\partial_x)\check\psi_{\sigma\ell}(x,t):\,, \tag{4a}$$

$$H^z_K = J^z_{\ell\ell}\, S^z_{\rm imp}\left(\frac{\sigma}{2} :\check\psi^\dagger_{\sigma\ell}(0,t)\check\psi_{\sigma\ell}(0,t):\right)$$
$$+ e^{i\bar\ell eVt} J^z_{\ell\bar\ell}\, S^z_{\rm imp}\left(\frac{\sigma}{2}\check\psi^\dagger_{\sigma\ell}(0,t)\check\psi_{\sigma\bar\ell}(0,t)\right), \tag{4b}$$

$$H^\perp_K = J^\perp_{\ell\ell}\, S^\sigma_{\rm imp}\left(\tfrac{1}{2}\check\psi^\dagger_{\bar\sigma\ell}(0,t)\check\psi_{\sigma\ell}(0,t)\right)$$
$$+ e^{i\bar\ell eVt} J^\perp_{\ell\bar\ell}\, S^\sigma_{\rm imp}\left(\tfrac{1}{2}\check\psi^\dagger_{\bar\sigma\ell}(0,t)\check\psi_{\sigma\bar\ell}(0,t)\right); \tag{4c}$$

and we bosonize according to $\mathcal{H}^0_\ell$, with $H^{z,\perp}_{\rm K}$ taken as the interaction terms. We follow the same standard bosonization prescription as we did for the junction problem [1], $\check{\psi}_{\sigma\ell}(x,t) = \frac{1}{\sqrt{2\pi a}} F_{\sigma\ell}(t) e^{-i\phi_{\sigma\ell}(x,t)}$, and in terms of the bosons the Hamiltonian density for the leads takes the usual form (the Klein factors, $F_{\sigma\ell}$, drop out from these terms):

$$\mathcal{H}^0 = \sum_\ell \mathcal{H}^0_\ell = \frac{v_{\rm F}}{4\pi} \sum_{\substack{\sigma=\uparrow,\downarrow \\ \ell={\rm L,R}}} :[\partial_x \phi_{\sigma\ell}(x,t)]^2: . \tag{5}$$

Using the same standard physically motivated rotated boson basis, $\phi_{\sigma\ell} = (\phi_c + \sigma\phi_s + \ell\phi_l + \sigma\ell\phi_{sl})/2$, as we did for the simple junction [1], the noninteracting Hamiltonian density retains its quadratic form:

$$\mathcal{H}^0 = \frac{v_{\rm F}}{4\pi} \sum_{\nu=c,s,l,sl} :[\partial_x \phi_\nu(x,t)]^2: . \tag{6}$$

Let us postpone the discussion of $H^z_{\rm K}$, and proceed to bosonize the "perpendicular" part of the Kondo term. The first part is the intralead one, or lead-nonmixing, and it is present also in the standard two-channel Kondo model, while the second part is interlead, or lead-mixing, and is responsible for transport as can already be seen from the voltage dependence (we keep the time and space dependence of the bosonic fields implicit for the sake of brevity):

$$\begin{aligned} H^\perp_{\rm K} = {} & \frac{J^\perp_{\ell\ell}}{2\pi a} S^\sigma_{\rm imp} \left(\frac{1}{2} F^\dagger_{\bar\sigma\ell} e^{i\phi_{\bar\sigma\ell}} F_{\sigma\ell} e^{-i\phi_{\sigma\ell}} \right) \\ & + e^{i\bar\ell eVt} \frac{J^\perp_{\ell\bar\ell}}{2\pi a} S^\sigma_{\rm imp} \left(\frac{1}{2} F^\dagger_{\bar\sigma\ell} e^{i\phi_{\bar\sigma\ell}} F_{\sigma\bar\ell} e^{-i\phi_{\sigma\bar\ell}} \right). \end{aligned} \tag{7}$$

We now change to the rotated boson basis and being careful of not combining vertex operators with opposite signs we introduce $\tilde n$ factors in the same manner as in our consistent BdB treatment of the simple junction problem [1]; notice as well that we are also introducing the $1/2$ factors associated with consistent boundary conditions (CBCs) [1]. We get

$$\begin{aligned} H^\perp_{\rm K} = {} & \frac{J^\perp_{\ell\bar\ell}}{2\pi a} \frac{\tilde n_c \tilde n^\ell_l}{2} S^\sigma_{\rm imp} (F^\dagger_{\bar\sigma\ell} F_{\sigma\ell} e^{i\bar\sigma\phi_s} e^{i\bar\sigma\ell\phi_{sl}}) \\ & + e^{i\bar\ell eVt} \frac{J^\perp_{\ell\bar\ell}}{2\pi a} \frac{\tilde n_c \tilde n^{\bar\sigma\ell}_{sl}}{2} S^\sigma_{\rm imp} (F^\dagger_{\bar\sigma\ell} F_{\sigma\bar\ell} e^{i\bar\sigma\phi_s} e^{i\ell\phi_l}), \end{aligned} \tag{8}$$

where almost all possible $\tilde n$ factors, i.e.,

$$\tilde n_c \equiv e^{i\phi_c/2} e^{-i\phi_c/2}/\sqrt{2}, \tag{9a}$$

$$\tilde n^\sigma_s \equiv e^{i\sigma\phi_s/2} e^{-i\sigma\phi_s/2}/\sqrt{2}, \tag{9b}$$

$$\tilde n^\ell_l \equiv e^{i\ell\phi_l/2} e^{-i\ell\phi_l/2}/\sqrt{2}, \tag{9c}$$

$$\tilde n^{\sigma\ell}_{sl} \equiv e^{i\sigma\ell\phi_{sl}/2} e^{-i\sigma\ell\phi_{sl}/2}/\sqrt{2}, \tag{9d}$$

appear except for the ones from the *spin* sector.

The same as in the case of the simple barrier junction, we do not expect the Klein factors to modify the physics. We treat them as we did in that case [28,29] by identifying relations between different bilinears of *original* and *new* Klein factors and fixing the four arbitrary phases; see Eqs. (16a)–(16d) from Ref. [1]. The rest of the Klein-factor relations can be derived from these [30]. In particular, for the intralead terms, we need

$$F^\dagger_{\uparrow\rm R} F_{\downarrow\rm R} = F^\dagger_{sl} F^\dagger_s , \tag{10a}$$

$$F^\dagger_{\uparrow\rm L} F_{\downarrow\rm L} = F_{sl} F^\dagger_s , \tag{10b}$$

$$F^\dagger_{\downarrow\rm R} F_{\uparrow\rm R} = F_s F_{sl} , \tag{10c}$$

$$F^\dagger_{\downarrow\rm L} F_{\uparrow\rm L} = F_s F^\dagger_{sl} , \tag{10d}$$

whereas for the interlead terms we need

$$F^\dagger_{\uparrow\rm R} F_{\downarrow\rm L} = F^\dagger_s F^\dagger_l , \tag{10e}$$

$$F^\dagger_{\uparrow\rm L} F_{\downarrow\rm R} = F_l F^\dagger_s , \tag{10f}$$

$$F^\dagger_{\downarrow\rm L} F_{\uparrow\rm R} = F_l F_s , \tag{10g}$$

$$F^\dagger_{\downarrow\rm R} F_{\uparrow\rm L} = F_s F^\dagger_l . \tag{10h}$$

Replacing the Klein factors and expanding $H^\perp_{\rm K}$ explicitly one arrives at

$$\begin{aligned} H^\perp_{\rm K} = {} & \frac{J^\perp_{\rm RR}}{2\pi a} \frac{\tilde n_c \tilde n^+_l}{2} (S^+_{\rm imp} F_s F_{sl} e^{-i\phi_s} e^{-i\phi_{sl}} \\ & + F^\dagger_{sl} F^\dagger_s e^{i\phi_s} e^{i\phi_{sl}} S^-_{\rm imp}) \\ & + \frac{J^\perp_{\rm LL}}{2\pi a} \frac{\tilde n_c \tilde n^-_l}{2} (S^+_{\rm imp} F_s F^\dagger_{sl} e^{-i\phi_s} e^{i\phi_{sl}} \\ & + F_{sl} F^\dagger_s e^{i\phi_s} e^{-i\phi_{sl}} S^-_{\rm imp}) \\ & + e^{-ieVt} \frac{J^\perp_{\rm RL}}{2\pi a} \frac{\tilde n_c}{2} (\tilde n^-_{sl} S^+_{\rm imp} F_s F^\dagger_l e^{-i\phi_s} e^{i\phi_l} \\ & + \tilde n^+_{sl} F^\dagger_s F^\dagger_l e^{i\phi_s} e^{i\phi_l} S^-_{\rm imp}) \\ & + e^{ieVt} \frac{J^\perp_{\rm LR}}{2\pi a} \frac{\tilde n_c}{2} (\tilde n^+_{sl} S^+_{\rm imp} F_l F_s e^{-i\phi_s} e^{-i\phi_l} \\ & + \tilde n^-_{sl} F_l F^\dagger_s e^{i\phi_s} e^{-i\phi_l} S^-_{\rm imp}). \end{aligned} \tag{11}$$

It is easy to notice that the impurity spin and the lead degrees of freedom associated with the *spin* sector always appear together in the combination $S^+_{\rm imp} F_s e^{-i\phi_s}$ and its Hermitian conjugate.

B. Toulouse limit and completion of the square

It is natural to describe the strong-coupling limit between the impurity and the electrons by looking for a transformation that binds those two degrees of freedom together as a single one. As shown by E&K, that is achieved by the following transformation (the boson field is evaluated at the position of the impurity):

$$U = e^{i\gamma_s \phi_s S^z_{\rm imp}} . \tag{12}$$

It follows by simple algebra that U is unitary and commutes with all the Klein factors and vertex operators (notice that one defines U so that no *point splitting* is involved when applying it). Using the spin algebra, $[S^\pm_{\rm imp}, S^z_{\rm imp}] = \mp S^\pm_{\rm imp}$, and the Baker-Campbell-Hausdorff (BCH) formula, $e^{-B} A e^B =$

$A + [A,B] + \frac{1}{2!}[[A,B],B] + \cdots$, we find

$$U S^{\pm}_{\rm imp} U^\dagger = S^{\pm}_{\rm imp} e^{\pm i\gamma_s \phi_s}, \tag{13a}$$

$$U S^{z}_{\rm imp} U^\dagger = S^{z}_{\rm imp}. \tag{13b}$$

Therefore, the perpendicular Kondo term in the Hamiltonian transforms as $\tilde{H}^{\perp}_{\rm K} = U H^{\perp}_{\rm K} U^\dagger$, which with the simplifying choice of $\gamma_s = 1$ to absorb the *spin-sector* vertex into the impurity, and further defining $d^\dagger = S^{+}_{\rm imp} F_s$ (so that $d^\dagger d = S^z + 1/2$), takes the form

$$\begin{aligned}\tilde{H}^{\perp}_{\rm K} = {}& \frac{J^{\perp}_{\rm RR}}{2\pi a}\frac{\tilde{n}_c \tilde{n}^{+}_l}{2}(d^\dagger F_{sl} e^{-i\phi_{sl}} + F^\dagger_{sl} e^{i\phi_{sl}} d) \\ & + \frac{J^{\perp}_{\rm LL}}{2\pi a}\frac{\tilde{n}_c \tilde{n}^{-}_l}{2}(d^\dagger F^\dagger_{sl} e^{i\phi_{sl}} + F_{sl} e^{-i\phi_{sl}} d) \\ & + e^{-ieVt}\frac{J^{\perp}_{\rm RL}}{2\pi a}\frac{\tilde{n}_c}{2}(\tilde{n}^{-}_{sl} d^\dagger F^\dagger_l e^{i\phi_l} - \tilde{n}^{+}_{sl} F^\dagger_l e^{i\phi_l} d) \\ & - e^{ieVt}\frac{J^{\perp}_{\rm LR}}{2\pi a}\frac{\tilde{n}_c}{2}(\tilde{n}^{+}_{sl} d^\dagger F_l e^{-i\phi_l} - \tilde{n}^{-}_{sl} F_l e^{-i\phi_l} d). \end{aligned} \tag{14}$$

Note that no $\tilde{n}^{\pm}_s$ factors appeared in these terms; they would appear in the interlead cotunneling terms of $H^z_{\rm K}$, but we follow S&H and set the coupling constants of those terms to zero as part of the definition of the Toulouse limit. So we need to discuss the intralead part of $H^z_{\rm K}$ and the kinetic terms. Let us examine further the effects of the E&K transformation. The transformation of a boson derivative is given by

$$\begin{aligned} U\partial\phi_s(x)U^\dagger &= \partial\phi_s(x) - i\gamma_s S^z_{\rm imp}[\partial\phi_s(x),\phi_s(0)] + \cdots \\ &= \partial\phi_s(x) - 2\pi\gamma_s S^z_{\rm imp}\delta(x), \end{aligned} \tag{15}$$

where we used $Ae^B = e^B(A + [A,B] + \cdots)$, which follows immediately from the BCH formula and the equal-time commutator $[\phi_\nu(x),\partial\phi_{\nu'}(y)] = 2\pi i\delta(x-y)\delta_{\nu\nu'}$. In terms of the corresponding fermions, via debosonization, this shift translates into a change of boundary conditions and thus U is sometimes called a "boundary-condition changing operator" [31,32]. When $\gamma_s = 1$ this gives (up to a conventional sign) an Abelian version of the shift that Affleck and Ludwig use to "complete the square" and absorb the impurity in a redefinition of the "spin density" at the infrared fixed point [24]. On the one hand, for the *spin-sector* part of the kinetic energy, we use this shift and obtain

$$\begin{aligned}\tilde{\mathcal{H}}^0_{\nu=s} &= \frac{v_{\rm F}}{4\pi}\big[\partial\phi_s(x) - 2\pi\gamma_s S^z_{\rm imp}\delta(x)\big]^2 \\ &= \frac{v_{\rm F}}{4\pi}[\partial\phi_s(x)]^2 - v_{\rm F}\gamma_s S^z_{\rm imp}\partial\phi_s(0) + \gamma_s^2 v_{\rm F}\frac{\pi}{4}\delta(0). \end{aligned} \tag{16}$$

On the other hand, for the parallel Kondo terms we get

$$\begin{aligned}\tilde{H}^z_{\rm K} = {}& \frac{1}{4\pi}J^z_{\rm avg} S^z_{\rm imp}\big[\partial\phi_s(0) - 2\pi\gamma_s S^z_{\rm imp}\delta(0)\big] \\ & + \frac{1}{8\pi}\big(J^z_{\rm RR} - J^z_{\rm LL}\big) S^z_{\rm imp}\partial\phi_{sl}, \end{aligned} \tag{17}$$

where $J^z_{\rm avg} = (J^z_{\rm RR} + J^z_{\rm LL})/2$. For the Toulouse limit one considers the symmetric case, $J^z_{\rm RR} = J^z_{\rm LL}$, and sets $J^z_{\rm avg} \to 4\pi v_{\rm F}\gamma_s = 4\pi v_{\rm F}$. Combining these two results and disregarding constant energy shifts, one has

$$U\big(\mathcal{H}^0_{\nu=s} + H^z_{\rm K}\big)U^\dagger = \frac{v_{\rm F}}{4\pi}[\partial\phi_s(x)]^2. \tag{18}$$

In summary, all the parallel Kondo terms were either set to zero or absorbed into the kinetic term and dropped out from the problem.

Finally, the local-field term is not affected by the transformation procedure and is written as

$$H_{\rm field} = -h\, S^z_{\rm imp} = -h\,(d^\dagger d - 1/2). \tag{19}$$

C. Debosonization

The kinetic terms are easily written back in terms of fermions, becoming similar to the original kinetic terms of the model. The only nontrivial part of the Hamiltonian that we need to debosonize and discuss carefully is the "perpendicular" Kondo terms. The final result for the lead-symmetric case reads

$$\begin{aligned}\tilde{H}^{\perp}_{\rm K} = {}& J_{\rm ra}\frac{\tilde{n}_c\tilde{n}^{+}_l}{2}(d^\dagger\psi_{sl}(0) + \psi^\dagger_{sl}(0)d) \\ & + J_{\rm ra}\frac{\tilde{n}_c\tilde{n}^{-}_l}{2}(d^\dagger\psi^\dagger_{sl}(0) + \psi_{sl}(0)d) \\ & - J_{\rm er}\frac{\tilde{n}_c\tilde{n}^{+}_{sl}}{2}(d^\dagger\psi_l(0) + \psi^\dagger_l(0)d) \\ & - J_{\rm er}\frac{\tilde{n}_c\tilde{n}^{-}_{sl}}{2}(\psi^\dagger_l(0)d^\dagger + d\psi_l(0)), \end{aligned} \tag{20}$$

where (cf. Fig. 1)

$$J_{\rm ra} = J^{\perp}_{\ell\bar{\ell}}/\sqrt{2\pi a} \quad \text{and} \quad J_{\rm er} = J^{\perp}_{\ell\bar{\ell}}/\sqrt{2\pi a}\,; \tag{21}$$

and later we will compactly denote

$$J_\pm = \frac{J_{\rm ra}\tilde{n}_c\tilde{n}^{\pm}_l}{4v_{\rm F}} \quad \text{and} \quad T_\pm = \frac{J_{\rm er}\tilde{n}_c\tilde{n}^{\pm}_{sl}}{4v_{\rm F}}. \tag{22}$$

The $\tilde{n}^{\pm}_\nu$'s defined in Eq. (9) are now viewed as square roots of local fermionic densities at the site of the impurity. While writing Eq. (20), we have already gauged away the time dependence from the coupling constants so that $\mu_{\nu=l} = -(eV)$ and all other chemical potentials are zero. This is achieved by using the transformation $\psi_l(x,t) = e^{ieV(t-x/v_{\rm F})}\check{\psi}_l(x,t)$ where $\check{\psi}_\nu = \frac{1}{\sqrt{2\pi a}}F_\nu e^{-i\phi_\nu}$ are the debosonized fields, as was done for the simple junction [1].

IV. TRANSPORT CALCULATIONS

In order to solve for the transport characteristics, we derive an expression for the current according to $\hat{I} = \partial_t\frac{\Delta N}{2} = i[H,\frac{\Delta N}{2}] = i[H^{\perp}_{\rm K}, N_{\nu=l}]$, which gives $I = \langle\hat{I}\rangle$ as (notice $[\tilde{n}^{\pm}_l, N_{\nu=l}] = 0$)

$$I = -i\,J_{\rm er}\frac{\tilde{n}_c}{2}[\tilde{n}^{-}_{sl}(\langle d^\dagger\psi^\dagger_l\rangle - \langle\psi_l d\rangle) - \tilde{n}^{+}_{sl}(\langle\psi^\dagger_l d\rangle - \langle d^\dagger\psi_l\rangle)], \tag{23}$$

and the problem reduces to finding those matrix elements.

A. Conventional approach

In the *conventional* BdB program, the boson exponentials that result after changing basis are freely recombined and as a result they simply disappear. This is equivalent, in the expressions above which already incorporate CBCs that are conventionally not discussed, to replacing $\tilde{n}_\nu^\pm \to 1$ everywhere [cf. Eq. (9)].

To calculate the necessary Green's function elements, using the same *local action* scheme and principal-value regularization (cf. Ref. [33]) as we did for the case of the junction [1], we adopt the following Keldysh-Nambu spinor basis (with the frequencies restricted to the positive semiaxis only in order to avoid double counting),

$$\Psi(\omega) = (\psi_l^-(\omega)\ \ \psi_l^+(\omega)\ \ \psi_l^{\dagger-}(\bar{\omega})\ \ \psi_l^{\dagger+}(\bar{\omega})\ \ d^-(\omega)\ \ d^+(\omega)\ \ d^{\dagger-}(\bar{\omega})\ \ d^{\dagger+}(\bar{\omega})\ \ \psi_{sl}^-(\omega)\ \ \psi_{sl}^+(\omega)\ \ \psi_{sl}^{\dagger-}(\bar{\omega})\ \ \psi_{sl}^{\dagger+}(\bar{\omega}))^T.$$

Let us define $s_\nu(\omega) \equiv \tanh\frac{\omega-\mu_\nu}{2T_{\rm emp}}$ and $\bar{s}_\nu(\omega) \equiv \tanh\frac{\omega+\mu_\nu}{2T_{\rm emp}}$, where $T_{\rm emp}$ is the temperature that is taken to be uniform (and that we will set to zero for the most part). The local inverse Green's function for the junction, $G^{-1}(\omega)/2v_{\rm F}$, is thus given by the following matrix:

$$\begin{pmatrix}
is_l & -is_l+i & 0 & 0 & T_+ & 0 & T_- & 0 & 0 & 0 & 0 & 0\\
-is_l-i & is_l & 0 & 0 & 0 & -T_+ & 0 & -T_- & 0 & 0 & 0 & 0\\
0 & 0 & i\bar{s}_l & -i\bar{s}_l+i & -T_- & 0 & -T_+ & 0 & 0 & 0 & 0 & 0\\
0 & 0 & -i\bar{s}_l-i & i\bar{s}_l & 0 & T_- & 0 & T_+ & 0 & 0 & 0 & 0\\
T_+ & 0 & -T_- & 0 & \omega+h & 0 & 0 & 0 & -J_+ & 0 & -J_- & 0\\
0 & -T_+ & 0 & T_- & 0 & -\omega-h & 0 & 0 & 0 & J_+ & 0 & J_-\\
T_- & 0 & -T_+ & 0 & 0 & 0 & \omega-h & 0 & J_- & 0 & J_+ & 0\\
0 & -T_- & 0 & T_+ & 0 & 0 & 0 & -\omega+h & 0 & -J_- & 0 & -J_+\\
0 & 0 & 0 & 0 & -J_+ & 0 & J_- & 0 & is_{sl} & -is_{sl}+i & 0 & 0\\
0 & 0 & 0 & 0 & 0 & J_+ & 0 & -J_- & -is_{sl}-i & is_{sl} & 0 & 0\\
0 & 0 & 0 & 0 & -J_- & 0 & J_+ & 0 & 0 & 0 & i\bar{s}_{sl} & -i\bar{s}_{sl}+i\\
0 & 0 & 0 & 0 & 0 & J_- & 0 & -J_+ & 0 & 0 & -i\bar{s}_{sl}-i & i\bar{s}_{sl}
\end{pmatrix};$$

we also rescaled frequencies and the magnetic field with $2v_{\rm F}$ (alternatively, one can think we took $v_{\rm F} = 1/2$).

After finding the Green's functions of interest we replace $T_\pm \longmapsto J_{\rm er}/2$ and $J_\pm \longmapsto (J_{\rm ra} \pm K)/2$, where in the second one (in order to facilitate the comparison with previous results from the literature) we reintroduced the possible asymmetry between right and left leads, which stretching our notation is given by $K = (J_{\rm ra}^{\rm L} - J_{\rm ra}^{\rm R})/2$. Combining these results one gets the following expression for the current:

$$I = \int_0^{+\infty} \frac{J_{\rm er}^2\left[\left(J_{\rm er}^2+K^2\right)\left(\omega^2+J_{\rm ra}^4\right)+h^2J_{\rm ra}^2\right][s_l(\omega)-\bar{s}_l(\omega)]}{\omega^4+\left[J_{\rm ra}^4+\left(J_{\rm er}^2+K^2\right)^2-2h^2\right]\omega^2+\left[J_{\rm ra}^2\left(J_{\rm er}^2+K^2\right)+h^2\right]^2}\frac{d\omega}{2\pi}. \tag{24}$$

This expression is completely equivalent to the one S&H reported in their original work. [See Eqs. (7) and (8) of Ref. [20] and match their notation to ours according to $\Gamma_a = \Gamma_1 + K^2$ where $\Gamma_1 = J_{\rm er}^2$, and $\Gamma_b = J_{\rm ra}^2$.] In particular, it is interesting to consider the case of zero magnetic field. One finds

$$I = \int_0^{+\infty} \frac{J_{\rm er}^2\left(J_{\rm er}^2+K^2\right)}{\omega^2+\left(J_{\rm er}^2+K^2\right)^2}[s_l(\omega)-\bar{s}_l(\omega)]\frac{d\omega}{2\pi}, \tag{25}$$

which is a rather peculiar result, since the dependence on $J_{\rm ra}$ has completely dropped out from the problem. This integral is elementary in the zero-temperature limit,

$$\begin{aligned}\lim_{T_{\rm emp}\to 0} I &= \frac{1}{\pi}\int_0^V \frac{J_{\rm er}^2\left(J_{\rm er}^2+K^2\right)}{\omega^2+\left(J_{\rm er}^2+K^2\right)^2}d\omega\\ &= \frac{1}{\pi}J_{\rm er}^2\arctan\frac{V}{J_{\rm er}^2+K^2},\end{aligned} \tag{26}$$

and it can also be carried out at finite temperature in terms of digamma functions [34].

Let us focus back on the lead-symmetric case with $K = 0$. When there is no magnetic field, there is no dependence on $J_{\rm ra}$ in the conventional result and it applies to the case of $J_{\rm ra} = 0$ in particular. But in that case the structure of $\tilde{H}_{\rm K}^\perp$ resembles closely that of the tunneling term in a simple junction [1], with $\tilde{n}_{sl}^\pm$ playing the role that was played there by $\tilde{n}_s^\pm$ and $d^\dagger$ replacing $\psi_{sl}^\dagger$. Therefore, in this limit we know (based on our experience with the junction) how to take the $\tilde{n}$'s into account. And we thus know one should expect the consistent result to be rather different from the conventional one, except perhaps for small $J_{\rm er}$. Indeed, due to the presence of the $\tilde{n}$ factors in the consistent approach, the structure of the problem is that of a resonant level attached to a single lead. Because of the alternation of different $\tilde{n}$'s, there are no Majorana-like operators that could contribute to the transport and give a nonzero current (cf. Ref. [35]), unlike in the conventional approach. In other words, the expected consistent-approach

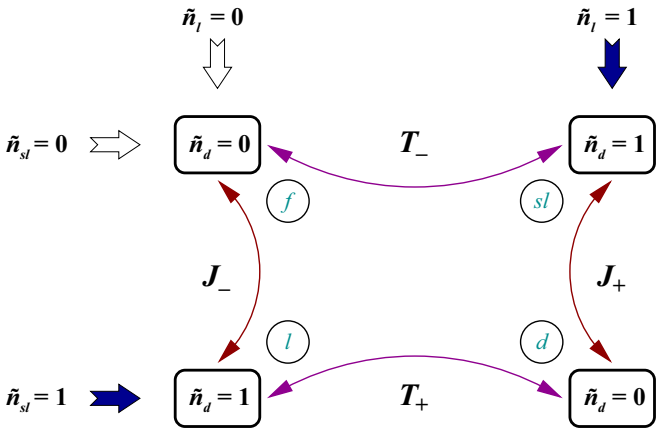

FIG. 2. Graphical representation of the states that contribute to transport. Intralead processes are indicated by the vertical arrows ($J_\pm$) that conserve $\tilde{n}_l$, while interlead processes are given by the horizontal arrows ($T_\pm$) that conserve $\tilde{n}_{sl}$. The circles indicate the state labels for the single-particle sector of an equivalent Gaussian problem that shares the exact same processes (see the discussion in the text).

result when $J_{\rm ra} = 0$ is simply $dI/dV = 0$ for any value of $J_{\rm er}$. It follows that we need to treat the $\tilde{n}$'s consistently for all values of $J_{\rm ra}$, but that requires additional insights.

B. Consistent approach

Let us turn again to the problem of finding the necessary expectation values, fully dressed by $\tilde{H}_{\rm K}^{\perp}$ as in Eq. (20), needed to compute the current as in Eq. (23). The challenge is to treat the factors $\tilde{n}_l^{\pm}$ and $\tilde{n}_{sl}^{\pm}$ consistently. This is a nontrivial problem, but we are nevertheless able to provide an *ad hoc* solution. In order to achieve that, we start by studying the local Hilbert space at the impurity site and the structure of the processes that take place; this is graphically summarized in Fig. 2.

Let us consider the possible sets of eigen-expectation-values of $\tilde{n}_{d,l,sl} = 0,1$ (cf. Ref. [1]). There are eight combinations in total, but those in which they add up to an odd number constitute isolated states that are not connected by processes in $\tilde{H}_{\rm K}^{\perp}$ and, in particular, do not contribute to transport. That leaves only four states as depicted in the figure.

From our study of the simple junction [1], we know that the physical content of the $\tilde{n}$ factors is actually to avoid contractions between normal and anomalous terms; in the present case, however, those are allowed but when and only when $J_{\rm ra}$ and $J_{\rm er}$ processes alternate. By considering processes at different orders of perturbation in $\tilde{H}_{\rm K}^{\perp}$, one can conclude that we can achieve the same set of processes, and also avoid the presence of anomalous terms, by modifying the *anomalous terms* in Eq. (20) according to the following prescription:

$$\begin{aligned} d^\dagger &\longrightarrow \tilde{f}^\dagger, \\ \psi_l^\dagger &\longrightarrow -\tilde{\psi}_{sl}, \\ \psi_{sl}^\dagger &\longrightarrow \tilde{\psi}_l, \end{aligned}$$

while not adjusting those same fields (only renaming them by adding twiddles) in the *regular terms*, and removing all the $\tilde{n}$ factors everywhere. In particular, one can check processes to fourth order in perturbation, when there are combinations in which all possible vertexes enter and the state of the system goes around full circle; cf. Fig. 2. We verified all these processes are in one-to-one correspondence in both formulations. This mapping is also argued for in a different way in the Appendix, by studying some exactly solvable limits of the two-lead Kondo model.

The mapping has to be applied to a version of $\tilde{H}_{\rm K}^{\perp}$ previous to that in Eq. (20), that is already debosonized but in which the factors of $e^{\pm ieVt}$ still appear explicitly in the interlead terms and can be removed ulteriorly. We are thus lead to consider

$$\begin{aligned} \tilde{H}_{\rm K}^{\perp} = &\frac{J_{\rm ra}^+}{2}(\tilde{d}^\dagger\tilde{\psi}_{sl}(0) + \tilde{\psi}_{sl}^\dagger(0)\tilde{d}) \\ &+ \frac{J_{\rm ra}^-}{2}(\tilde{f}^\dagger\tilde{\psi}_l(0) + \tilde{\psi}_l^\dagger(0)\tilde{f}) \\ &- \frac{J_{\rm er}^+}{2}(\tilde{d}^\dagger\tilde{\psi}_l(0) + \tilde{\psi}_l^\dagger(0)\tilde{d}) \\ &- \frac{J_{\rm er}^-}{2}(\tilde{f}^\dagger\tilde{\psi}_{sl}(0) + \tilde{\psi}_{sl}^\dagger(0)\tilde{f}), \end{aligned} \tag{27}$$

where the $\pm$ superscripts are used simply to keep track of what was the corresponding superscript in the now-absent $\tilde{n}_s^{\pm}$'s of the different terms, but in the calculations the two couplings will be taken as having equal numerical values. The $e^{\pm ieVt}$ factors were removed from the couplings by using again a time-dependent gauge transformation. The choice of gauge transformation is this time not unique. We adopted the following symmetric choice: $\mu_l = \mu_f = -eV/2$ and $\mu_{sl} = \mu_d = eV/2$. Another choice could have been $\mu_l = \mu_f = -eV$ and the other two zero; we checked that these and other choices are all equivalent. We need to stress that we introduced the $\tilde{\psi}$ notation to emphasize an important interpretational difference with Eq. (20): after applying the prescribed mapping, and even though we kept similar notations for the fields, there is no connection left to the physical sectors of the theory.

We also want to consider the local magnetic-field term which is naturally rewritten in a symmetric way (see the Appendix):

$$\tilde{H}_{\rm field} = -h\,(\tilde{d}^\dagger\tilde{d} + \tilde{f}^\dagger\tilde{f} - 1). \tag{28}$$

The current is given by

$$\begin{aligned} I = \langle\hat{I}\rangle = i\Bigg[&\frac{J_{\rm er}^-}{2}(\langle\tilde{\psi}_{sl}\tilde{f}^\dagger\rangle - \langle\tilde{f}\tilde{\psi}_{sl}^\dagger\rangle) \\ &+ \frac{J_{\rm er}^+}{2}(\langle\tilde{d}\tilde{\psi}_l^\dagger\rangle - \langle\tilde{\psi}_l\tilde{d}^\dagger\rangle)\Bigg]. \end{aligned} \tag{29}$$

The resulting calculation is straightforward. Using the spinor basis

$$\Psi(\omega) = (\tilde{\psi}_{sl}^- \quad \tilde{\psi}_{sl}^+ \quad \tilde{\psi}_l^- \quad \tilde{\psi}_l^+ \quad \tilde{d}^- \quad \tilde{d}^+ \quad \tilde{f}^- \quad \tilde{f}^+)^T \tag{30}$$

and adopting the same notations as for the conventional calculation, the local inverse Green's function for the junction is given by

$$G^{-1}(\omega)=2v_{\mathrm{F}}\begin{pmatrix} is_{sl} & -is_{sl}+i & 0 & 0 & J_+ & 0 & -T_- & 0\\ -is_{sl}-i & is_{sl} & 0 & 0 & 0 & -J_+ & 0 & T_-\\ 0 & 0 & is_l & -is_l+i & -T_+ & 0 & J_- & 0\\ 0 & 0 & -is_l-i & is_l & 0 & T_+ & 0 & -J_-\\ J_+ & 0 & -T_+ & 0 & \omega+h-V & 0 & 0 & 0\\ 0 & -J_+ & 0 & T_+ & 0 & -\omega-h+V & 0 & 0\\ -T_- & 0 & J_- & 0 & 0 & 0 & \omega+h+V & 0\\ 0 & T_- & 0 & -J_- & 0 & 0 & 0 & -\omega-h-V \end{pmatrix},$$

where it should be noticed that the voltage now enters explicitly also in the resonant-level-like diagonal-block action matrix elements corresponding to $\tilde{d}^\dagger$ and $\tilde{f}^\dagger$. The voltage was written here absorbing a factor of $e/2$ only to keep the matrix expression short; it will be reinserted below. The final expression for the current is

$$I=\int_{-\infty}^{+\infty}\frac{d\omega}{2\pi}\frac{2\left(J_{\mathrm{ss}}^2-J_{\mathrm{ds}}^2\right)(\omega+h)^2}{\left[(\omega+h)^2-J_{\mathrm{ds}}^2-(eV/2)^2\right]^2+4J_{\mathrm{ss}}^2(\omega+h)^2}[s_l(\omega)-s_{sl}(\omega)], \tag{31}$$

where $J_{\mathrm{ss/ds}}=(J_{\mathrm{ra}}^2\pm J_{\mathrm{er}}^2)/4$ are the sum and the difference of the squares of the couplings, respectively. Notice that only the squares of the couplings enter into the final expression, which means that all the $\tilde{n}$'s would have appeared squared as well. As anticipated, the current vanishes if either J_{ra} or J_{er} is zero. The integral can be done in general, but it is simpler and more illuminating in the zero-temperature limit. Using $d(s_l-s_{sl})/dV=(e/2)d(s_l-s_{sl})/d(eV/2)\to e[\delta(\omega+eV/2)+\delta(\omega-eV/2)]$, we directly write down an expression for the zero-temperature differential conductance,

$$\begin{aligned}\frac{dI}{dV}=&\sum_{s=\pm1}\frac{2(e/2\pi)\left(J_{\mathrm{ss}}^2-J_{\mathrm{ds}}^2\right)(h+s\,eV/2)^2}{\left[(h+s\,eV/2)^2-J_{\mathrm{ds}}^2-(eV/2)^2\right]^2+4J_{\mathrm{ss}}^2(h+s\,eV/2)^2}\\&+\int_{-\infty}^{+\infty}\frac{d\omega}{2\pi}\frac{4e(eV/2)\left(J_{\mathrm{ss}}^2-J_{\mathrm{ds}}^2\right)\left[(\omega+h)^2-J_{\mathrm{ds}}^2-(eV/2)^2\right](\omega+h)^2}{\left\{\left[(\omega+h)^2-J_{\mathrm{ds}}^2-(eV/2)^2\right]^2+4J_{\mathrm{ss}}^2(\omega+h)^2\right\}^2}[s_l(\omega)-s_{sl}(\omega)].\end{aligned} \tag{32}$$

C. Comparison of results

In what follows we will illustrate the differences between the results obtained using the conventional and consistent approaches discussed in the previous two sections. We will do so mainly by considering the behavior of the differential conductance, first as a function of J_{er} and J_{ra} for specific values of h and eV as shown in Fig. 3 and then by looking at its behavior as a function of h and eV for specific values of J_{er} and J_{ra} as shown in Figs. 4, 5, and 6. The physical interpretation and plausibility of the consistent-approach results will be presented as well.

Figure 3 shows the values of the differential conductance for voltage $V=0$ and field $h=v_{\mathrm{F}}$ as a function of J_{er} while fixing $J_{\mathrm{ra}}=1$, or vice versa. We denote J_{er} and J_{ra} by J in the two cases, respectively. The two cases produce completely identical plots at zero voltage, as can be seen from the symmetry of Eqs. (24) and (31). From these expressions, one can also see that for the current and differential conductance derived using the consistent scheme, the symmetry under exchange of J_{er} and J_{ra} continues to be present also at finite voltage. On the other hand, the symmetry is absent when one puts $h=0$ for any value of voltage in the conventional expression and further the transport is dictated solely by the value of J_{er}. It is to be noted that the order of limits for J_{er}, J_{ra}, V, and h going to zero is in general important and needs to be treated carefully, as can be seen by a direct study of the expressions for the current.

From a diagrammatic point of view, one would have expected the conventional and consistent plots in Fig. 3 to be asymptotically equivalent for small J. An expansion in the couplings of the zero-voltage dI/dV derived from Eqs. (24) and (31) shows that, unlike the case of a junction [1] or the Ising limit considered in the Appendix, there is no contribution to the current in the lowest order. That is the order at which the two calculations would have matched (as indeed happens for the simple junction and the Ising limit). The next order is $O(J_{\mathrm{er}}^2J_{\mathrm{ra}}^2)$, which is the first nonvanishing order for the differential conductance and the first one consistent with the emerging $J_{\mathrm{er}}\leftrightarrow J_{\mathrm{ra}}$ duality of the problem at the Toulouse point that was discussed above. At this order, the conventional calculation is larger than the consistent one by a factor of 2; which is the same factor that one finds for the (same) next-to-lowest order of the expansion of the consistent calculation as compared with the exact direct results in the cases of both the junction and the Ising limit. Interestingly, as can be seen from the comparison of the dI/dV results for $J_{\mathrm{er}}=J_{\mathrm{ra}}$, the two calculational schemes yield, at zero voltage, results that are identical except for the aforementioned factor of 2. Motivated by these two observations, we also provided in Fig. 3 the conventional result scaled by a factor of $1/2$.

Although the tails do not match in Fig. 3, the two ways of calculating give the same result as J (i.e., J_{er} or J_{ra}) goes to zero while the other one (i.e., J_{ra} or J_{er}, respectively) is nonzero. However, similarly to the case of a simple junction [1], the

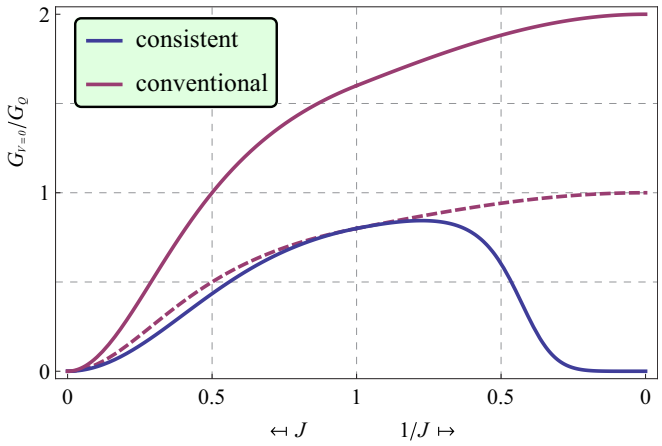

FIG. 3. Comparison of the differential conductance for the two-lead Kondo junction, $G = dI/dV$ (in units of the single-channel conductance quantum, $G_Q = e^2/h$), calculated according with the conventional procedure or using our consistent scheme. The plot is at zero applied voltage and finite magnetic field ($h = v_F$). Notice the convention used for the horizontal axis in order to cover the full range of J (see also the corresponding plot for the simple junction [1]). Here, differently from previous sections, J stands for either J_{er} or J_{ra} while the other (J_{ra} or J_{er}, respectively) is set to 1; the resulting plots are identical for both cases at zero voltage. The dashed line gives for comparison the conventional result divided by a factor of 2.

results are different for finite J, the difference being most marked for large J. While the consistent conductance first increases and then falls down, eventually going to zero as $J \to \infty$, the conventional conductance continues to grow with increasing J and approaches the value $2e^2/h$.

One can gain some additional insights by appealing to physical arguments. The current is obviously zero if $J_{er} = 0$, but also if $J_{er} \to \infty$ due to the formation of a resonating-tunneling state that will block other electrons from approaching the junction (the same as what happens for a simple junction [1], since those arguments are not affected by the fact that tunneling now involves also spin flip). Therefore, a nonzero current requires the interlead exchange coupling to take some intermediate value. The physical picture is similar but more involved concerning the intralead couplings. If $J_{ra} = 0$, for instance, then the parallel Kondo terms which reach their maximal value at the Toulouse point (measured in terms of phase shifts) promote the formation of a strongly bound "static doublet" between an electron at each side and the impurity. Such a bound state "sits" at the location of the junction and Pauli-blocks the passage of a current: since electrons tunnel with spin flip, there is always one bound-state electron already occupying the site with the same spin projection that the tunneling electron would have either before or after tunneling. If $J_{ra} \to \infty$, in the opposite limit, then a complicated resonating-exchange state would form instead, but again the current would be blocked because other electrons would be blocked from approaching the junction (similarly as for $J_{er} \to \infty$). As a result, a steady-state current requires intermediate values of both inter- and intralead couplings.

In all the limits that involve strong coupling, the intuitive physical picture discussed above does not agree with the results of the conventional calculation, but it does with the consistent calculation in which the $\tilde{n}$'s are properly taken into account. This is a strong validation for the need to manipulate and debosonize models consistently after the initial bosonization. Additionally, it should also be remarked that the consistent conductance never exceeds the value of one single-channel quantum of conductance ($G_Q \equiv e^2/h$). This is also an emergent property at the nonequilibrium Toulouse point in addition to the $J_{er} \leftrightarrow J_{ra}$ transport duality, both of which are indicated by physical arguments along the lines discussed above.

It is interesting to take a more systematic look at the variation of the differential conductance with applied field and voltage. In Fig. 4 we show contour color maps of dI/dV for the conventional and consistent calculational schemes, while fixing the Kondo couplings to the symmetric choice $J_{er} = 1 = J_{ra}$. For additional clarity, in Fig. 5 we show also two half-plane cuts of the differential conductance maps: a vertical one at constant magnetic field, $h/v_F = 5$, and a horizontal one at constant voltage, $eV/v_F = 5$. For these cuts, the horizontal axis is defined in terms of either $x = eV/h$ (dashed lines) or $x = h/eV$ (solid lines), respectively. As is clearly evident from the figures, the effects of field and voltage turn out to be exactly equivalent in the conventional calculation (as seen from the 90° rotational symmetry of the first contour plot or from the complete overlap of the two "conventional" traces in the cuts). However, the consistent calculation yields inequivalent dependencies on field and voltage.

Both ways of calculating show a splitting of the zero-bias differential-conductance anomaly due to the finite magnetic field when plotting as a function of voltage, but the peaks are sharper and more asymmetric in the consistent calculation. The contrast between the two results is even greater at finite applied voltage when plotting as a function of magnetic field. In the consistent case and for low applied voltages, only part of the zero-bias anomaly splits, while a relatively broad relic of it remains pinned at zero bias. As a result the contour plots are star- or butterfly-shaped, instead of being cross-shaped as in the conventional calculation. For small x (as compared with J_{er} and J_{ra}), the differential conductance can additionally be described as showing a small "deep" developing right after/before the "peak" when plotting as a function of voltage or field, respectively. In other words, besides the "ridges" in the contour maps for $|h| = 0, |eV|$, there are also "furrows" at $|2h| = |eV|$ which are absent from the conventional calculation. This can be seen analytically by looking at the small-coupling expansion of the differential conductance.

To take a closer look at the central part of the contour maps, we plot in Fig. 6 horizontal and vertical cuts going through $h = V = 0$ (solid and dashed lines, respectively). In the conventional calculation, the differential conductance reaches the maximum value of $2G_Q$ at zero field and bias, and decreases towards zero as either of them increases (once again, the symmetry of the behavior with h and V make the solid and dashed lines coincide with each other). On the other hand, the consistently calculated differential conductance reaches a maximum value of G_Q at the origin—only half as tall—and it decreases towards zero differently with field or with applied voltage, with the latter being the slowest decay and the only one

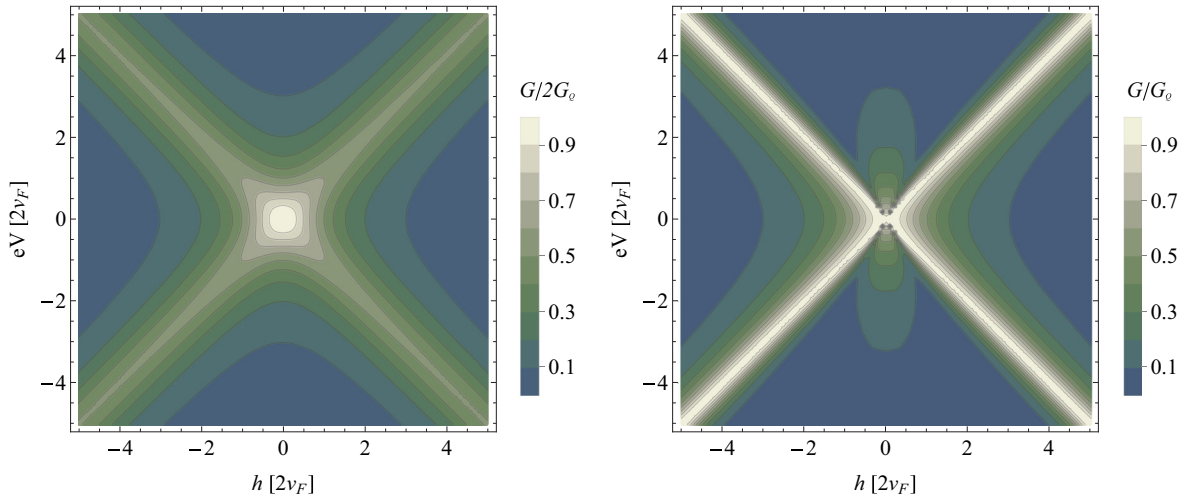

FIG. 4. Contour color maps of the differential conductance, $G = dI/dV$, in units of (twice) the single-channel conductance quantum as a function of applied field and voltage. The two panels compare the conventional calculation (left panel, in units of $2G_Q$) and our consistent calculation (right panel, in units of G_Q) for the case of $J_{\rm er} = 1 = J_{\rm ra}$. While, conventionally, applying a field or a finite voltage have the same effect, that is not the case in a consistent calculation.

of these four curves not following a steepest descent. Notice in addition, from the contour maps, that only along the diagonal ridges would the differential conductance not go to zero asymptotically. Let us point out that the way the asymptotic values are approached in all cases is as a power law instead of the expected logarithmic tail [23,36]. This is a peculiarity of the Toulouse limit, in which the voltage or local magnetic field can never be larger than the parallel Kondo couplings and the bandwidth is infinite. So the standard argument in which such energy scales stop the renormalization-group flow of the couplings does not apply. Moreover, already in the conventional framework and for equilibrium situations, a standardly formulated renormalization-group scheme [37] is not compatible with the nature of the Toulouse-limit fixed-point manifold, which calls for a careful reformulation [29,38].

Let us also stress and comment on the differences between the ways in which applied voltage and temperature enter in both calculations. In the conventional calculation, both enter into the expression for the charge current, Eq. (24), through the thermal factors $s_l(\omega)$ and $s_{sl}(\omega)$ only, but not via the kernel multiplying them (the spectral function of a Majorana

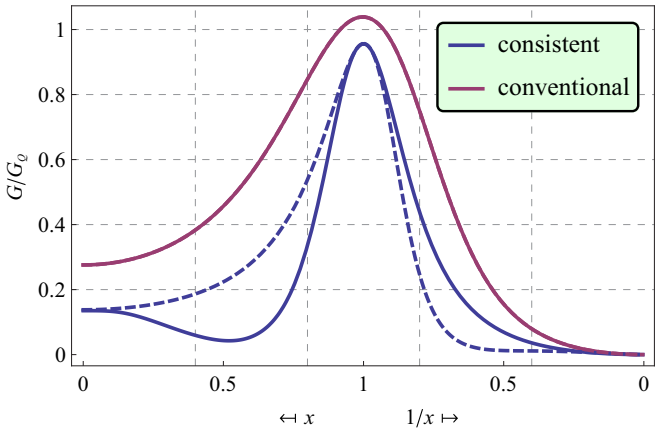

FIG. 5. Differential conductance for the two-lead Kondo junction, $G = dI/dV$ (in units of the single-channel conductance quantum), calculated according with the conventional procedure (in red) or using our consistent scheme (in blue). The plots are either at a finite constant field ($h = 5v_{\rm F}$) and as a function of applied voltage (dashed lines), or at a finite constant applied voltage ($eV = 5v_{\rm F}$) and as a function of magnetic field (solid lines). For the conventional calculation, both plots are identical and the dashed line is covered by the solid one. Notice the convention used for the horizontal axis in order to cover the full range of x (defined in terms of either $x = eV/h$ or $x = h/eV$, with the field that is kept constant being the one in the denominator).

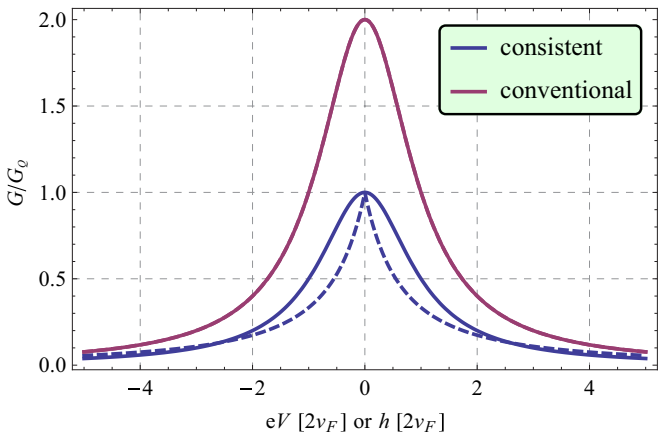

FIG. 6. Differential conductance for the two-lead Kondo junction, $G = dI/dV$ (in units of the single-channel conductance quantum), calculated according with the conventional procedure (in red) or using our consistent scheme (in blue). The plots are either at a zero field and as a function of applied voltage (dashed lines), or at a zero voltage and as a function of magnetic field (solid lines). For the conventional calculation, both plots are identical and the dashed line is covered by the solid one.

fermion in this case). The latter is independent of both eV and $T_{\rm emp}$, which is ascribed to the quadratic nature of the problem at the solvable point [34]. Only as one moves away from the solvable point, the voltage and temperature will explicitly enter into the kernel of the integrand [39]. This is in contradistinction to the consistent calculation in which the voltage enters explicitly into the kernel of Eq. (31), but not the temperature. Thus, not only voltage and magnetic field, but also voltage and temperature, interplay differently as compared with the previously accepted, conventional results for the nonequilibrium Toulouse point. If one were to imagine that these kernels capture the Kondo-resonance part of the spectral function of some parent Anderson-type impurity model, one could see how the resonance reacts to applied field or voltage. On the one hand, in both calculations the resonance would shift from zero frequency with magnetic field. On the other hand, the resonance would not depend on voltage in the conventional picture, but it would split with the applied drain-source bias in the consistent picture. The latter would be in agreement with experimental results and the accepted phenomenological picture of Kondo transport out of equilibrium [40] (and as first predicted in Ref. [41]).

V. CONCLUSION AND FINAL REMARKS

In the companion work [1], we presented a *consistent bosonization-debosonization* program in which we introduced the $\tilde{n}$ factors, defined here in Eq. (9), to assist in making the results consistent after performing transformations in the bosonic language and later debosonizing models that include terms with single-point non-normal-ordered operators. How these factors should be treated depends on the physical setup being considered and needs to be studied on a case by case basis. Sometimes the conventional way (i.e., $\tilde{n} \to 1$ for all of them) could be the one consistent with the problem, but other times the consistent treatment is different. Moreover, this treatment can be connected to the choice of boundary conditions that is dictated by the problem (cf. Ref. [1]).

We applied these ideas here to the important case of quantum impurity problems. In particular, we focused our attention on the two-lead Kondo model of a junction out of equilibrium. By considering certain regimes of the problem, we were able to argue that the conventional way of calculating does not produce consistent results, while a different treatment of the $\tilde{n}$ factors seems to fix those problems (as it did for the case of the simple junction problem [1]). Moreover, the calculations can then be carried out in the full regime of parameters of the system. This way, the key insights of the work by S&H (and also by E&K) can be retained and the calculations fixed to produce consistent results (our method of solution was *ad hoc* and there is no exact solution to refer to as in the case of the junction, but we do know it interpolates between consistent limits). We thus were able to make a number of predictions for the transport characteristics of the two-lead Kondo model that can, in principle, be looked for in experiments.

Certainly, more work should be done along this line following the developments of the literature of the past two decades, and we are already exploring some directions. To name but a few: (i) the consistent solution can be explored further, including additional aspects of transport (such as the noise spectrum and possibly thermal transport), alternatives such as charge sensing [42], and also the thermodynamics; (ii) one can study ac-drive effects that are realizable in experiments [43,44]; (iii) a study of multiterminal models would provide new insights, cf. Refs. [31,45]; (iv) perturbation around the solvable Toulouse point needs to be considered anew, cf. Refs. [39,46]; (v) connections to other approaches such as boundary CFT can bring in synergy [47,48], showing for example how to possibly extend those methods to nonequilibrium transport problems; (vi) ditto for approaches that exploit the connections to integrability [49] or to renormalization ideas [50]; (vii) one could combine our approach with a finite-size bosonization analysis to further bridge with CFT and numerical renormalization ideas [28]. The list can go on (even though we restricted it to quantum impurity problems only). Given the continued challenge posed by the need to better understand strongly correlated quantum systems out of equilibrium, the consistent Toulouse-point solution will play an important role as a reference case for a class of problems in which a lot is still not well understood and there is a lack of exact results to guide the theoretical developments.

ACKNOWLEDGMENTS

We acknowledge the hospitality of the Kavli Institute for Theoretical Physics and the Aspen Center for Physics where part of this research was done. C.J.B. thanks A. Schiller for several past discussions of his work on quantum-impurity physics. N.S. acknowledges the hospitality of the University of Cologne while she studied Refs. [28,34,51] and thanks A. Rosch for providing her an opportunity to present a series of pedagogical blackboard talks on that topic.

APPENDIX: SOME EXACTLY SOLVABLE LIMITS

In the following, we consider two different limits that can be rigorously treated via exact direct calculations. They further motivate the prescription mapping discussed in the main text to solve for the transport within the consistent approach.

1. $\hat{x}$-axis Ising limit

We call the Ising limit of the anisotropic Kondo model that in which all the spin-spin exchange interactions take place along a single axis. We will choose it to be the $\hat{x}$ axis (as is often done for the transverse-field Ising model). The virtue of this limit is that it is exactly solvable: the electrons still interact with the impurity but the latter does not have dynamics (i.e., no spin flips take place along the $\hat{x}$ axis). As a result, all one has to do is to solve for each possible impurity orientation and average over the results (this is reminiscent of the treatment of the boundary sine-Gordon model that one obtains at the solvable point of the problem of a classical impurity in a Tomonaga-Luttinger liquid [31,52]; cf. Ref. [53]). When the impurity is frozen, the only remaining degrees of freedom are the electronic ones and the problem becomes Gaussian and thus exactly solvable in a direct way. We shall keep the $\hat{z}$ axis as the quantization axis for the electrons, as this will show some structure that will help us understand how to deal with the full two-lead Kondo model in the language of Abelian bosonization.

In the zero-field case, and setting in Eq. (1) all the non-x couplings to zero, $J^y_{\ell\ell'}, J^z_{\ell\ell'} = 0$, we are left with (the time dependence is implicit)

$$H = \sum_{\sigma,\ell}\left(\int \mathcal{H}^0_\ell\, dx + H^x_{\rm K}\right), \tag{A1a}$$

$$\mathcal{H}^0_\ell = \psi^\dagger_{\sigma\ell}(x)(-iv_{\rm F}\partial_x)\psi_{\sigma\ell}(x), \tag{A1b}$$

$$H^x_{\rm K} = J^x_{\ell\ell'}\, S^x_{\rm imp}\left(\frac{1}{2}\psi^\dagger_{\bar\sigma\ell}(0)\psi_{\sigma\ell'}(0)\right), \tag{A1c}$$

where we have made use of the relation $2S^x_{\rm imp}S^x_{\rm elec} = S^x_{\rm imp}(S^+_{\rm elec} + S^-_{\rm elec})$. Hermiticity requires $J^x_{\rm RL} = J^x_{\rm LR} = J^x_{\rm er}$. It is a simple exercise to solve the model directly and find a closed expression for the differential conductance (for brevity, we do not quote that result here).

We are interested in bosonizing, changing boson basis, and debosonizing in the *same way* as we did for the full model (gauging the voltage in and out from the couplings also in the same way). Of course, no unitary transformation is required this time since $S^x_{\rm imp}$ commutes with the Hamiltonian and thus plays a simple spectator role. The Kondo part of the Hamiltonian is finally rewritten as (all fields are at time t and $x = 0$)

$$\begin{aligned} H^x_{\rm K} = {} & J^x_{\rm RR}\frac{\tilde n_c\tilde n_l^+}{2}S^x_{\rm imp}(\psi^\dagger_{sl}\psi^\dagger_s + \psi_s\psi_{sl}) \\ & - J^x_{\rm LL}\frac{\tilde n_c\tilde n_l^-}{2}S^x_{\rm imp}(\psi^\dagger_s\psi_{sl} + \psi^\dagger_{sl}\psi_s) \\ & + J^x_{\rm er}\frac{\tilde n_c\tilde n_{sl}^+}{2}S^x_{\rm imp}(\psi^\dagger_s\psi^\dagger_l + \psi_l\psi_s) \\ & - J^x_{\rm er}\frac{\tilde n_c\tilde n_{sl}^-}{2}S^x_{\rm imp}(\psi^\dagger_l\psi_s + \psi^\dagger_s\psi_l). \end{aligned} \tag{A2}$$

One could now set all $\tilde n \to 1$ and proceed conventionally to calculate the differential conductance. The result is that the expression differs from the direct calculation in a way that parallels what we discussed for a simple junction [1]. In particular, a small-coupling expansion shows that the results match to lowest order, $O[(J^x_{\rm er})^2]$, but the conventional result is twice bigger than the direct one at next-leading order, as was the case for the simple junction. Therefore, one needs to treat the $\tilde n$'s more carefully.

The practical problem that arises is that the factors $\tilde n^\pm_l$ and $\tilde n^\pm_{sl}$ introduce complicated dynamics into the Hamiltonian because there are linear terms in $\psi^{[\dagger]}_l$ and $\psi^{[\dagger]}_{sl}$ present as well. From our study of the simple junction [1], we know that the physical content of these factors is actually to avoid contractions between regular and anomalous terms of the same type (i.e., inter- or intralead). Here the situation is more complicated because regular and anomalous terms of a given type can be combined provided there is an intervening term of the other type, and vice versa. One can check this conclusion order by order via a matching of perturbative expansions as we did for the case of the simple junction [1].

But since the present problem is directly solvable in terms of the original fermions, we know there exists a way of organizing the perturbation theory as if the model was purely Gaussian. We shall thus focus on the structure of the terms while comparing new and original fermions. We do that by looking at the four Klein factor relations [see Eqs. (10a)–(10h)] that involve $F^\dagger_s$: (i) for the regular terms, $F_{sl}F^\dagger_s = F^\dagger_{\uparrow\rm L}F_{\downarrow\rm L}$ and $F_lF^\dagger_s = F^\dagger_{\uparrow\rm L}F_{\downarrow\rm R}$; and (ii) for the anomalous terms, $F^\dagger_{sl}F^\dagger_s = F^\dagger_{\uparrow\rm R}F_{\downarrow\rm R}$ and $F^\dagger_lF^\dagger_s = -F^\dagger_{\uparrow\rm R}F_{\downarrow\rm L}$. The other four are just the Hermitian conjugates of these.

A first observation is that in terms of the original fermions there are no anomalous terms present in the model; see Eq. (A1). This prompts us to attempt a mapping in which we do not change the regular terms but "regularize" the anomalous ones. Notice that while $F^\dagger_s$ appears in all four terms, no single original Klein factor appears four times; while $F^\dagger_{\uparrow\rm L}$ repeats in the regular terms, $F^\dagger_{\uparrow\rm R}$ does in the anomalous ones. A second observation is that the pair of spin-down original Klein factors repeat in regular and anomalous terms, but they exchange roles as to which one goes in the intralead process and which in the interlead process in each case.

These two observations indicate that we can achieve the same perturbative processes (and, as a bonus, avoid the presence of anomalous terms) by modifying *only* the anomalous terms according to the following prescription:

$$\begin{aligned} \psi^\dagger_s &\longrightarrow \tilde\psi^\dagger_z, \\ \psi^\dagger_l &\longrightarrow -\tilde\psi_{sl}, \\ \psi^\dagger_{sl} &\longrightarrow \tilde\psi_l, \end{aligned} \tag{A3}$$

and removing all the $\tilde n$ factors. To keep the same phase conventions as we used for the matching of Klein factor bilinears, we also need to introduce a minus sign in all the terms (this is not essential as the current is not sensitive to it). Explicitly, one has

$$\begin{aligned} H^x_{\rm K} = {} & \frac{1}{2}J^x_{\rm R}S^x_{\rm imp}(\tilde\psi^\dagger_l\tilde\psi_z + \tilde\psi^\dagger_z\tilde\psi_l) \\ & + \frac{1}{2}J^x_{\rm L}S^x_{\rm imp}(\tilde\psi^\dagger_s\tilde\psi_{sl} + \tilde\psi^\dagger_{sl}\tilde\psi_s) \\ & + \frac{1}{2}J^x_{\rm er}S^x_{\rm imp}(\tilde\psi^\dagger_{sl}\tilde\psi_z + \tilde\psi^\dagger_z\tilde\psi_{sl}) \\ & + \frac{1}{2}J^x_{\rm er}S^x_{\rm imp}(\tilde\psi^\dagger_l\tilde\psi_s + \tilde\psi^\dagger_s\tilde\psi_l), \end{aligned} \tag{A4}$$

and, trivially since the $\tilde\psi$'s can be put in one-to-one correspondence with the original fermions in Eq. (A1), all the results will be the same as in the direct solution. We stress that, even though we kept the notation with s, l, and sl, these are different fermions and there is no direct connection left to the physical sectors of the theory (we introduced the $\tilde\psi$ notation to emphasize this point).

2. Flat-band limit

If one introduces a lattice discretization, the flat-band limit is the limit of zero hopping between sites. Then all sites in each band are independent fermionic degrees of freedom, except for the sites at x_0, the location of the impurity, which are connected by the tunneling terms in the Hamiltonian. We could consider this limit for the Toulouse-point Hamiltonian with its Kondo part given by Eq. (20) or for the BdB-mapped $\hat x$-axis-Ising Hamiltonian corresponding to Eq. (A2). Both

yield equivalent models in the flat-band limit; for brevity, we frame our presentation around the second case. Taking the band energies to be zero, we introduce the notation $\psi_\nu^\dagger(x_0) \to c_\nu^\dagger$ for $\nu = s,l,sl$ (or $d^\dagger \to c_s^\dagger$ in the first case) to emphasize the lattice nature of the problem and the sector of the Hamiltonian containing $x = x_0$ turns into the following three-site model (taking the expectation value of the "spectator" impurity spin and absorbing it in redefined coupling constants),

$$H_{3s} = J_{ra}^a n_l^+ (c_{sl}^\dagger c_s^\dagger + c_s c_{sl}) - J_{ra}^r n_l^- (c_s^\dagger c_{sl} + c_{sl}^\dagger c_s) + J_{er}^a n_{sl}^+ (c_s^\dagger c_l^\dagger + c_l c_s) - J_{er}^r n_{sl}^- (c_l^\dagger c_s + c_s^\dagger c_l). \quad \text{(A5)}$$

Since now we are dealing with lattice fermions, we can directly identify $\tilde{n}_\nu \to n_\nu$.

This model has an eight-state Hilbert space split into two particle-number-parity sectors. The states with even number of particles are all disconnected degenerate states with zero energy. The states with odd particle number hybridize and can be diagonalized (using exact diagonalization) into four eigenstates with energies $\pm\sqrt{-b/2 \pm \sqrt{b^2/4 - c}}$ where $b = -[(J_{ra}^a)^2 + (J_{ra}^r)^2 + (J_{er}^a)^2 + (J_{er}^r)^2]$ and $c = (J_{ra}^a J_{ra}^r - J_{er}^a J_{er}^r)^2$.

Applying the prescribed changes for the anomalous terms, this Hamiltonian turns into the equivalent of Eq. (A4), which is now a four-site model with no anomalous terms,

$$H_{4s} = - J_{ra}^a (\tilde{c}_z^\dagger \tilde{c}_l + \tilde{c}_l^\dagger \tilde{c}_z) - J_{ra}^r (\tilde{c}_s^\dagger \tilde{c}_{sl} + \tilde{c}_{sl}^\dagger \tilde{c}_s) - J_{er}^a (\tilde{c}_z^\dagger \tilde{c}_{sl} + \tilde{c}_{sl}^\dagger \tilde{c}_z) - J_{er}^r (\tilde{c}_l^\dagger \tilde{c}_s + \tilde{c}_s^\dagger \tilde{c}_l). \quad \text{(A6)}$$

This model conserves particle number and, in the single-particle sector, its spectrum coincides with the odd sector of H_{3s} (cf. Fig. 2). Moreover, the same conclusion remains true when we introduce a local magnetic field as in Eqs. (19) or (28), appropriately rewritten. This serves as a check of how to correctly normalize the local-field term after the mapping. In other words, the Hamiltonian matrices in those two sectors are unitary equivalent,

$$P_{\text{odd}} H_{3s} P_{\text{odd}} \underset{U}{\equiv} P_{1p} H_{4s} P_{1p}\,. \quad \text{(A7)}$$

Due to the absence of interactions in H_{4s}, its many-particle physics can be calculated in terms of a Green's function for a single fermion injected into an empty band [54], and thus the single-particle sector is the crucial one to determine the full dynamics. Notice, in addition, that the way this kind of Green's functions at the bare level enter into the transport calculations of the main text is via their inverses. As such, the propagator of any hybridized local or flat-band degree of freedom will not require independent regularization and will inherit its causal properties (i.e., its Keldysh structure [33]) from other extended-band degrees of freedom; and thus the difference between "empty-band" and "degenerate-gas" Green's functions does not enter the calculations. Thus, for those physical properties whose calculation requires only the two-point Green's functions and, by extension, only the single-particle sector, the Hamiltonian mapped via the prescription should work fine. And in the particular example above we were able to show explicitly that the single-particle sector of the mapped model reproduces the nontrivial part of the original spectrum.

In summary, the mapping we prescribed for the anomalous terms works in both cases, namely the linear- and the flat-band limits. In the case of the two-lead-Kondo-model Toulouse point, we encountered two linear-band and one local degrees of freedom, which is a combination of these two cases we just discussed. One can resort to neither bosonization nor exact diagonalization to prove the mapping rigorously, but it is nevertheless justified on physical grounds as a combination of these two limits and as argued also in terms of processes in the main text.

[1] N. Shah and C. J. Bolech, Consistent bosonization-debosonization. I. A resolution of the nonequilibrium transport puzzle, Phys. Rev. B **93**, 085440 (2016).

[2] J. Kondo, Resistance minimum in dilute magnetic alloys, Prog. Theor. Phys. **32**, 37 (1964).

[3] Kondo effect—40 years after the discovery, J. Phys. Soc. Jpn. **74** (2005) (special issue).

[4] D. L. A. Cox and A. Zawadowski, *Exotic Kondo Effects in Metals: Magnetic Ions in a Crystalline Electric Field and Tunnelling Centres* (Taylor & Francis, London, 1999); Exotic Kondo effects in metals: Magnetic ions in a crystalline electric field and tunnelling centres, Adv. Phys. **47**, 599 (1998).

[5] A. C. Hewson, *The Kondo Problem to Heavy Fermions* (Cambridge University Press, Cambridge, 1993).

[6] N. Andrei, Diagonalization of the Kondo Hamiltonian, Phys. Rev. Lett. **45**, 379 (1980).

[7] P. B. Wiegmann, Towards an exact solution of the Anderson model, Phys. Lett. A **80**, 163 (1980).

[8] N. Kawakami and A. Okiji, Exact expression of the ground-state energy for the symmetric Anderson model, Phys. Lett. A **86**, 483 (1981).

[9] N. Andrei and C. Destri, Solution of the Multichannel Kondo Problem, Phys. Rev. Lett. **52**, 364 (1984).

[10] C. J. Bolech and N. Andrei, Solution of the Two-Channel Anderson Impurity Model: Implications for the Heavy Fermion UBe_{13}, Phys. Rev. Lett. **88**, 237206 (2002); Solution of the multichannel Anderson impurity model: Ground state and thermodynamics, Phys. Rev. B **71**, 205104 (2005).

[11] A. A. Abrikosov, Electron scattering on magnetic impurities in metals and anomalous resistivity effects, Physics **2**, 5 (1965).

[12] S. E. Barnes, New method for the Anderson model, J. Phys. F: Met. Phys. **6**, 1375 (1976); New method for the Anderson model. II. The $U = 0$ limit, **7**, 2637 (1977).

[13] Piers Coleman, New approach to the mixed-valence problem, Phys. Rev. B **29**, 3035 (1984).

[14] H. Hafermann, C. Jung, S. Brener, M. I. Katsnelson, A. N. Rubtsov, and A. I. Lichtenstein, Superperturbation solver for quantum impurity models, Europhys. Lett. **85**, 27007 (2009).

[15] E. Muñoz, C. J. Bolech, and S. Kirchner, Universal Out-of-Equilibrium Transport in Kondo-Correlated Quantum Dots: Renormalized Dual Fermions on the Keldysh Contour, Phys. Rev. Lett. **110**, 016601 (2013).

[16] A. Georges, G. Kotliar, W. Kruth, and M. J. Rozenberg, Dynamical mean field theory of strongly correlated fermion systems and the limit of infinite dimensions, Rev. Mod. Phys. **68**, 13 (1996).

[17] D. Goldhaber-Gordon, H. Shtrikman, D. Mahalu, D. Abusch-Magder, U. Meirav, and M. A. Kastner, Kondo effect in a single-electron transistor, Nature (London) **391**, 156 (1998).

[18] S. M. Cronenwett, T. H. Oosterkamp, and L. P. Kouwenhoven, A tunable Kondo effect in quantum dots, Science **281**, 540 (1998).

[19] L. H. Yu and D. Natelson, The Kondo effect in C_{60} single-molecule transistors, Nano Lett. **4**, 79 (2004).

[20] A. Schiller and S. Hershfield, Exactly solvable nonequilibrium Kondo problem, Phys. Rev. B **51**, 12896 (1995).

[21] V. J. Emery and S. Kivelson, Mapping of the two-channel Kondo problem to a resonant-level model, Phys. Rev. B **46**, 10812 (1992).

[22] Ph. Nozières and A. Blandin, Kondo effect in real metals, J. Phys. Fr. **41**, 193 (1980).

[23] A. Kaminski, Yu. V. Nazarov, and L. I. Glazman, Universality of the Kondo effect in a quantum dot out of equilibrium, Phys. Rev. B **62**, 8154 (2000).

[24] I. Affleck, Conformal field theory approach to the Kondo effect, Acta Phys. Pol. B **26**, 1869 (1995) (lecture given at the XXXVth Cracow School of Theoretical Physics, Zakopane, Poland, June 4–14, 1995).

[25] Y. Imry and R. Landauer, Conductance viewed as transmission, Rev. Mod. Phys. **71**, S306 (1999).

[26] Ya. M. Blanter and M. Büttiker, Shot noise in mesoscopic conductors, Phys. Rep. **336**, 1 (2000).

[27] B. Doyon and N. Andrei, Universal aspects of nonequilibrium currents in a quantum dot, Phys. Rev. B **73**, 245326 (2006).

[28] J. von Delft, G. Zaránd, and M. Fabrizio, Finite-Size Bosonization of 2-Channel Kondo Model: A Bridge between Numerical Renormalization Group and Conformal Field Theory, Phys. Rev. Lett. **81**, 196 (1998); G. Zaránd and J. von Delft, Analytical calculation of the finite-size crossover spectrum of the anisotropic two-channel Kondo model, Phys. Rev. B **61**, 6918 (2000).

[29] C. J. Bolech and A. Iucci, Mapping of the Anisotropic Two-Channel Anderson Model onto a Fermi-Majorana Biresonant Level Model, Phys. Rev. Lett. **96**, 056402 (2006); A. Iucci and C. J. Bolech, Bosonization approach to the mixed-valence two-channel Kondo problem, Phys. Rev. B **77**, 195113 (2008).

[30] Yu-Wen Lee and Yu-Li Lee, Kondo effects in quantum dots at large bias, Phys. Rev. B **65**, 155324 (2002).

[31] A. O. Gogolin, A. A. Nersesyan, and A. M. Tsvelik, *Bosonization and Strongly Correlated Systems* (Cambridge University Press, Cambridge, 1998).

[32] K. D. Schotte and U. Schotte, Tomonaga's model and the threshold singularity of x-ray spectra of metals, Phys. Rev. **182**, 479 (1969); I. Affleck and A. W. W. Ludwig, The Fermi edge singularity and boundary condition changing operators, J. Phys. A: Math. Gen. **27**, 5375 (1994); J. Ye, Solution of the two-channel spin-flavor Kondo model, Phys. Rev. B **56**, R489 (1997); N. Shah and A. J. Millis, Dissipative Dynamics of an Extended Magnetic Nanostructure: Spin Necklace in a Metallic Environment, Phys. Rev. Lett. **91**, 147204 (2003).

[33] C. J. Bolech and T. Giamarchi, Point-Contact Tunneling involving Low-Dimensional Spin-Triplet Superconductors, Phys. Rev. Lett. **92**, 127001 (2004); Keldysh study of point-contact tunneling between superconductors, Phys. Rev. B **71**, 024517 (2005); C. J. Bolech and E. Demler, Observing Majorana Bound States in p-Wave Superconductors Using Noise Measurements in Tunneling Experiments, Phys. Rev. Lett. **98**, 237002 (2007); P. Kakashvili and C. J. Bolech, Time-loop formalism for irreversible quantum problems: Steady-state transport in junctions with asymmetric dynamics, Phys. Rev. B **78**, 033103 (2008).

[34] A. Schiller and S. Hershfield, Toulouse limit for the nonequilibrium Kondo impurity: Currents, noise spectra, and magnetic properties, Phys. Rev. B **58**, 14978 (1998).

[35] D. Roy, C. J. Bolech, and N. Shah, Majorana fermions in a topological superconducting wire out of equilibrium: Exact microscopic transport analysis of a p-wave open chain coupled to normal leads, Phys. Rev. B **86**, 094503 (2012).

[36] A. Rosch, J. Kroha, and P. Wölfle, Kondo Effect in Quantum Dots at High Voltage: Universality and Scaling, Phys. Rev. Lett. **87**, 156802 (2001).

[37] R. Shankar, Renormalization-group approach to interacting fermions, Rev. Mod. Phys. **66**, 129 (1994).

[38] A. L. Moustakas and D. S. Fisher, Prospects for non-Fermi-liquid behavior of a two-level impurity in a metal, Phys. Rev. B **53**, 4300 (1996).

[39] K. Majumdar, A. Schiller, and S. Hershfield, Nonequilibrium Kondo impurity: Perturbation about an exactly solvable point, Phys. Rev. B **57**, 2991 (1998).

[40] S. De Franceschi, R. Hanson, W. G. van der Wiel, J. M. Elzerman, J. J. Wijpkema, T. Fujisawa, S. Tarucha, and L. P. Kouwenhoven, Out-of-Equilibrium Kondo Effect in a Mesoscopic Device, Phys. Rev. Lett. **89**, 156801 (2002).

[41] Y. Meir, N. S. Wingreen, and P. A. Lee, Low-Temperature Transport through a Quantum Dot: The Anderson Model Out of Equilibrium, Phys. Rev. Lett. **70**, 2601 (1993).

[42] D. Berman, N. B. Zhitenev, R. C. Ashoori, and M. Shayegan, Observation of Quantum Fluctuations of Charge on a Quantum Dot, Phys. Rev. Lett. **82**, 161 (1999); C. J. Bolech and N. Shah, Prediction of the Capacitance Line Shape in Two-Channel Quantum Dots, *ibid.* **95**, 036801 (2005).

[43] Avraham Schiller and Selman Hershfield, Solution of an ac Kondo Model, Phys. Rev. Lett. **77**, 1821 (1996).

[44] A. Kogan, S. Amasha, and M. A. Kastner, Photoinduced Kondo satellites in a single-electron transistor, Science **304**, 1293 (2004); A. Kogan, S. Amasha, D. Goldhaber-Gordon, G. Granger, M. A. Kastner, and H. Shtrikman, Measurements of Kondo and Spin Splitting in Single-Electron Transistors, Phys. Rev. Lett. **93**, 166602 (2004).

[45] M. Fabrizio and A. O. Gogolin, Toulouse limit for the over-screened four-channel Kondo problem, Phys. Rev. B **50**, 17732 (1994); A. M. Tsvelik, Toulouse limit of the multichannel Kondo model, *ibid.* **52**, 4366 (1995); N. Shah and A. Rosch, Nonequilibrium conductance of a three-terminal quantum dot in the Kondo regime: Perturbative renormalization group study, *ibid.* **73**, 081309 (2006).

[46] D. G. Clarke, T. Giamarchi, and B. I. Shraiman, Curie and non-Curie behavior of impurity spins in quantum antiferromagnets, Phys. Rev. B **48**, 7070 (1993); A. M. Sengupta and A. Georges, Emery-Kivelson solution of the two-channel Kondo problem, *ibid.* **49**, 10020R (1994).

[47] I. Affleck, A current-algebra approach to the Kondo effect, Nucl. Phys. B **336**, 517 (1990); I. Affleck and A. W. W. Ludwig,

Critical-theory of overscreened Kondo fixed-points, *ibid.* **360**, 641 (1991).

[48] H. Johannesson, N. Andrei, and C. J. Bolech, Critical theory of the two-channel Anderson impurity model, Phys. Rev. B **68**, 075112 (2003); H. Johannesson, C. J. Bolech, and N. Andrei, Two-channel Anderson impurity model: Single-electron Green's function, self-energies, and resistivity, *ibid.* **71**, 195107 (2005).

[49] R. M. Konik, H. Saleur, and A. Ludwig, Transport in quantum dots from the integrability of the Anderson model, Phys. Rev. B **66**, 125304 (2002); P. Mehta and N. Andrei, Nonequilibrium Transport in Quantum Impurity Models: The Bethe Ansatz for Open Systems, Phys. Rev. Lett. **96**, 216802 (2006).

[50] F. B. Anders and A. Schiller, Real-Time Dynamics in Quantum-Impurity Systems: A Time-Dependent Numerical Renormalization-Group Approach, Phys. Rev. Lett. **95**, 196801 (2005); F. B. Anders, Steady-State Currents through Nanodevices: A Scattering-States Numerical Renormalization-Group Approach to Open Quantum Systems, *ibid.* **101**, 066804 (2008); S. Schmitt and F. B. Anders, Comparison between scattering-states numerical renormalization group and the Kadanoff-Baym-Keldysh approach to quantum transport: Crossover from weak to strong correlations, Phys. Rev. B **81**, 165106 (2010).

[51] J. von Delft and H. Schoeller, Bosonization for beginners—refermionization for experts, Ann. Phys. **7**, 225 (1998).

[52] C. L. Kane and M. P. A. Fisher, Transport in a One-Channel Luttinger Liquid, Phys. Rev. Lett. **68**, 1220 (1992); Transmission through barriers and resonant tunneling in an interacting one-dimensional electron gas, Phys. Rev. B **46**, 15233 (1992).

[53] F. Guinea, V. Hakim, and A. Muramatsu, Diffusion and Localization of a Particle in a Periodic Potential Coupled to a Dissipative Environment, Phys. Rev. Lett. **54**, 263 (1985); F. Guinea, Dynamics of a particle in an external potential interacting with a dissipative environment, Phys. Rev. B **32**, 7518 (1985).

[54] S. Doniach and E. H. Sondheimer, *Green's Functions for Solid State Physicists* (Imperial College Press, London, 1998).